Proceedings of the Fifth International Conference on Energy and Environment, Cairo, Egypt, 1996

ATMOSPHERIC TURBIDITY PARAMETERS IN THE HIGH POLLUTED SITE OF EGYPT

M.A.MOSALAM SHALTOUT, AND U.ALI RAHOMA
National Research Institute of Astronomy And Geophysics
Helwan -Cairo -Egypt

ABSTRACT: *Monthly variations of Linke, Angstrom and Schüepp turbidity coefficients and α exponent as well as the influence of climatic factor on them are analyzed. For each of these turbidity coefficients; calculated from measurements of broad band filters at Helwan, Egypt, desert climate, are reported. A linear regression model fitted to Angstrom's turbidity coefficint β and Linke turbidity factor L for Helwan. The calculation showed that, it is higher values of atmospheric turbidity coefficients due to, both the effect of air pollutants in the Helwan atmosphere from the four cement companies and some of Heavy industrial factories, and the effect of the former's desert climate.*

1- INTRODUCTION

The determination of the turbidity of the atmosphere is becoming increasingly important because it integrates the total loading of aerosol in the atmosphere. Atmospheric turbidity is generally recognized as the extinction of solar radiation by suspended particles with radii from about 100 to 10 000nm. Several turbidiy indices exist, namely the turbidity factor L of Linke and Boda (1922), the coefficient β of Angstrom (1929) and the factor B defined by Schüepp (1949). Each index is referred to the extinction at a specific wavelength or spectral interval: L to the spectrum, β to a wavelength of 1000nm and B to a wavelength of 500nm [1].

The solar radiation going through the atmosphere is partially absorbed by its constituents, partially reflected back to space and partially diffused, with the remaining reaching the ground as direct solar radiation. In a planetary scale, 17% of solar radiation is absorbed by the atmosphere, 30 % is reflected by the constituents of the atmosphere, and 53% reaches the surface of the earth, 31% of it as direct solar radiation and 22% as diffuse radiation [2]. In addition to the absorption and diffusion of solar radiation by the usual constituents of the atmosphere, aerosol particles and water (liquid or solid) also absorb and cause diffusion of solar radiation quite significantly. Therefore, the percentage of solar radiation finally reaching the surface of the ground depends on the turbidity of the atmospheric mass over the examined area and consequently on the concentration of the pollutant material. The reduction of the solar radiation is very important parameter when it refers to areas of increased atmospheric pollution such as big cities and industrial areas. The most interesting information is the fact that the atmosphere cannot clean itself when a specific limit of pollution has been reached [3].

Beginning at 300nm wavelength, there is a broad ozone (O_3) absorption band called the Hartly-Huggins band that extents from 350nm wavelength. The Capuis O_3 band then extends from 500 to 700nm wavelength. Water vapor (H_2O) absorption occurs

throughout the spectrum from 570nm to 2800nm. The strength of this absorption varies a great deal from wavelength to wavelength and is negligible at some wavelengths. Absorption from carbon dioxide (CO_2) occurs at several wavelengths longer than 1000nm, but the effect of CO_2 is relatively small. Narrow absorption features for oxygen (O_2) are dispersed throughout the spectrum with the major ones occurring near the 688 and 762nm wavelengths. Other absorbers shown that have very little effect are methane (CH_4) and nitrons oxide (N_2O), which absorb several wavelengths between 1900nm and the end of the plot, 2800nm [4].

Thus several ways to express atmospheric turbidity. In a global network, which is designed specifically to record long-term change in the aerosol loading of the atmosphere, it is preferable to use uniform particles and relative simple techniques so that comparable data are obtained. This manual will deal only with the determination of "aerosol optical thickness", from measurements of direct solar radiation made with sunphotometers and pyrheliometers[5].

2- DATA-BASE

For the study of the turbidity parameters in Helwan, Pyrheliometer data for the period June 1991-February 1996 were used. The observations were performed from sunset to sunrise, Local Standard Time (LST is 2h ahead of UT), whenever clouds were not present in the sight path.

The instrument used was Eppley pyrheliometer equipped with Schott filters OG530, RG630, and RG695. Their main characteristics (lower cut-off wavelength, and correction factor CF) are given in Table (1). A quartz filter was also used with a nominal cut-off wavelength of approximately 2800nm. The instrument was situated at the National Research Institute of Astronomy and Geophysics (NRIAG), 125 m above sea level, near the center of Helwan, a site known for high pollution level. Additionally, other necessary meteorological parameters, such as, temperature, relative humidity, wind speed, wind direction, cloud amount are available on daily routine basis, and sunshine duration.

Since the pyrheliometer measurements depend on weather and sky conditions, the number of observations is smaller in winter months and greater in summer months. The cloudiness at the time of the Pyrheliometer observations varied between zero and 2 Oktas. In the following, the turbidity parameters and related quantities are considered on a monthly basis.

3- DETERMINATION OF TURBIDITY WITH THE PYRHELIOMETER

Essentially, the pyrheliometric method consists of measuring solar intensity through broad-band filters. These are short-wave cut- off filters which transmit solar radiation of wavelengths greater than 530nm (Schott RG1), 630nm (Schott RG2), and 695nm (Schott RG8). The intensity measured behind the filters is normally used to compute turbidity with the methods described by Linke and Boda (1922), Angstrom (1929) and SchÜepp (1949). More detailed information is given in the IGY Instruction Manual (CSAGI, 1958) and the guide to Meteorological Instruction and Observing Practices (WMO,1971). The evaluation of broad-band filter data requires assumptions about the wavelength

dependence of the aerosol extinction coefficient. Extraterrestrial solar spectral irradiance data are needed. These data are at the present time only available with absolute accuracies of 2 per cent. Consequently, the accuracy of turbidity determinations is uncertain [4].

4-TURBIDITY MEASUREMENTS

Particulate matter suspended in the atmosphere interferes with the passage of light from the sun to the surface of the earth mostly by scattering it. Some of the scattered light will return back to space while the rest will appear as diffuse sky radiation. The scattering causes a certain degree of extinction of incoming light, characterized by an extinction function which can expressed as:

$$f(\lambda) = \beta\lambda^{-\alpha} \qquad (1)$$

where λ denotes the wavelength of the incoming light

β denotes the extinction coefficient at $\lambda=1\times10^{3}$nm (turbidity coefficient, and characterizing the aerosol content ,and

α denotes a factor (wavelength exponent) related to the size distribution of the particles responsible for the extinction = 1.3 suggested by Angstrom is currently accepted [6]. It is varies between 0 and 4.

The IGY Instruction Manual recommends the calculation of β using the RG630 filter and the clear filter measurements (i.e., 250nm to 630nm band).

Table (1): Values of λ_m and DR of the filters

Filter	OG530	RG630	RG695
λ_m (nm)	530	630	695
DR	1.082	1.068	1.042

The turbidity of the atmosphere is defined as the reduced transparency of the atmosphere, caused by absorption and scattering of radiation by solid or liquid particles other than clouds, held in suspension. As developed by Angstrom, the turbidity of the atmosphere is defined by β, the extinction coefficient at $\lambda=1\times10^{3}$nm, normally called the turbidity coefficient, and α, the wavelength exponent. β values less than 0.10 normally denote a very clear condition whereas values greater than 0.20 are a distinctly hazy condition.

The average value of α, which is dependent on the particle size distribution, was found by Angstrom to be about 1.3. The distribution of the size of the suspended particles greater than approximately 100nm and is governed by the formula:

$$dN = kr^{\gamma}\,dr \qquad (2)$$

where r is the particle radius

dN is the number of particles per unit volume in the size range r to r+dr

k is a constant dependent on the total number of particles, and

is an exponent which determines the "slope" of the particle number verus size curve. In practice r varies from about 3 to 5 typical value for polluted and clean atmospheres is 4.

These values were obtained by solving the Bouguer equation:

$$I_{\Delta\lambda} = I_{0\Delta\lambda} \exp [-m (\tau_{R\Delta\lambda} + \tau_{z\Delta\lambda} + \beta \lambda^{-\alpha}) \quad (3)$$

so that

$$\beta = 1/m \ \lambda^{\alpha} \ [\ln(I_{0\Delta\lambda} / I_{\Delta\lambda}) - m (\tau_{R\Delta\lambda} + \tau_{z\Delta\lambda})] \quad (4)$$

where $I_{0\Delta\lambda}$ denotes the spectral irradiance observed outside the atmosphere at the mean sun-earth distance in the wavelength band (spectral interval) $\Delta\lambda$

$I_{\Delta\lambda}$ denotes the spectral irradiance observed at the instrument in the same spectral interval

$\tau_{R\Delta\lambda}$ denotes the average extinction coefficient over the wavelength interval for molecules (Rayleigh scattering), *and*

$\tau_{z\Delta\lambda}$ denotes the average extinction coefficient over the wavelength interval for ozone.

m A simple expression by Kasten that we use for all solar zenith angles is given by:

$$m = [\cos\theta + 0.15 (93.885 - \theta)^{-1.253}]^{-1} \quad (6)$$

θ Solar zenith angle.

The Linke turbidity factor is estimated from the expression:

$$L = P(m) (\log I_{0\Delta\lambda} - \log I_{\Delta\lambda} - 2 \log s) \quad (5)$$

where, P(m) is a function of the optical mass m. The values of P(m) which are used in this study are obtained by the next formula which is the best fit of the values given by Coulson [7]. The extinction due to water vapor absorption can be ignored if the calculations are made only for those wavelength intervals λ<700nm.

The pyrheliometer technique to developed by SchÜepp (1949) requires replacing $\beta \lambda^{-\alpha}$ in equation (3) with B and using logarithms to the base 10 rather e. The same assumptions used in the determination of β apply to the determination of B with the exception that SchÜepp calculated the wavelength exponent α. This was done by calculating B values for two wavelengths intervals *530*<λ<630nm and 630<λ<695 nm. With this information,

$$\alpha = (\ln B_{530} - B_{630}) / (\lambda_{630} / \lambda_{5301}) \quad (7)$$

A turbidity coefficient value for 500 manometer can then be calculated:

$$\ln B_{500\,nm} = \alpha [\ln (\lambda_{630} / 500)] + \ln B_{\lambda 6} \quad (8)$$

Since the mean values of the two wavelength intervals cited above are relatively closed together, i.e. $\lambda_5 \approx$530nm and $\lambda_6 \approx$630nm, small errors in the computed B1, and B3

values can result in large variations in α. It is recommended that if all three filters are used, α should be determined from either of the band B pairs listed below:

1- I = $250 < \lambda < 2800$ nm
2- B1= $250 < \lambda < 530$ nm
3- B2 = $530 < \lambda < 630$ nm
4- B3 = $630 < \lambda < 695$ nm
5- B4 = $695 < \lambda < 2800$ nm

Since the average attenuation in the broad band intervals changes with air mass, the average wavelength for these intervals will also change. One method of selecting the average wavelength is assign it that wavelength for which the average attenuation $(\tau_R+\tau_z)^m$, has the same values as the $(\tau_R+\tau_z)$ value for m=1. For the broad band intervals (λ<500nm, λ<630nm, λ<695nm), the average Rayleigh+ozone attenuation is a function of the air mass [2]. These variation are shown in table (2).

Using the appropriate values for $(\tau_R+\tau_z)$ and $I_{0\Delta\lambda}$ B may be calculated for any of the spectral intervals from the following relationship:

$$B=[\, m.ln\, 1_0\ (ln\, I_{0\Delta\lambda}.s / I_{.1\lambda})]-(\tau_R+\tau_z) \qquad (9)$$

The factor s in the equation used to adjust the observed irradiance to the mean sun-earth distance. Angstrom (1929) determined that α has an average value of 1.3 when the

Table (2): The average of Rayleigh+Ozone attenuation function in air mass (m).

B	$\Delta\lambda$	$(\bar{\tau}_R + \bar{\tau}_z)$ $m=1$ $m=5$	$\bar{\lambda}$ $m=1$ $m=5$	$I_{0\Delta\lambda}$ cal cm^{-2} min^{-1}
B_1	$250<\lambda<530$ nm	0.164 0.117	396 430	0.558
B_2	$530<\lambda<630$ nm	0.051	591	0.270
B_3	$630<\lambda<695$ nm	0.028	662	0.150

wavelength is given in microns, so that

$$B= 1.069\beta \qquad (10)$$

In practice, α varies between about 0-4 depending on the particle size distribution (Angstrom, 1929; Bullrich, 1964), so the exact relationship between β and B requires an accurate knowledge of the wavelength exponent. In addition, determinations of β are generally made from pyrheliometer measurements of the radiation in relatively broad spectral intervals[6].

5- RESULTS AND DISCUSSION

Compare the weight of a 10 μm particle near the upper limit of those found suspended in the air and a 0.1μm particle which is near the lower limit. This range is high effective on visible light (between 300-800nm). The mode with the 10μm maximum are particles introduced to the atmosphere as solids from the surface of the earth and the seas, plus particles from the coagulation- condensation made which have grown larger and moved across the saddle between the mode into the larger size mode. These are primly Silicon, Iron, Aluminum, Sea salt, and Plant particles. Thus there is a dynamism that creates small particles, allows them to grow lager, and eventually allows the larger particles to be scavenged from the atmosphere by sedimentation (in the absence of precipitation), plus washout and rain out when there is precipitation. Much of the concur about particle matter in the atmosphere arises because particles of certain size ranges can be inhaled and retained by the human respiratory system. There is also concern because particle matter in the atmosphere absorbs and scatters incoming solar radiation. Helwan characterized by a high degree of turbidity, traffic in Helwan, but the turbidity must be due to the heavy industry surrounding the region. In the north-east and north of Helwan, cement industry is found in Toura, where the north-east and north winds transport the smoke and pollutants to Helwan atmosphere. Also, in the south iron-steel and cement industries are found, and the south wind transport the pollutants to Helwan, specially in winter. One of reason of turbidity in Helwan, its position relative to Cairo in the south-east direction and the effect of north or north-west wind. Cairo contains about one million cars work by the international combustion engines, produce $8x10^5$ Kg/year of the pollutants. Also $2x10^5$ Kg/year of lead is out from them, and increase by a rate of %2.6 per year. In the east of Cairo there is burning for $4x10^6$ Kg/year of the remains in the desert: The industrial region in the north of Cairo (Helwan), produce the following:- $2x10^9$ Kg/year of Carbon monoxide CO. $6.5x10^7$ Kg/year of Nitrogen oxides No_x. $2.5x10^8$ Kg/year of Hydrocarbons. The concentration of the pollutants in these two region are 1200 $\mu g/m^3$ [8].

In south of Cairo, there are four companies for cement industry, two in Toura and two in Helwan, about $2x10^5$ Kg of the pollutants and dust release from the chimneys every day. Using the electric precipitates and filters to collect the dust by efficiency about 99%, the high quantity of the released dust can be reduced, and in the same time the production of each company from cement can be increase by about %5. In 1980 the amount of the precipitant dust in Helwan area are $3.37x10^5$ $Kg/mile^2/month$, and led to hard environment condition.

The major source of pollution at Helwan are from three types of factories as following:-

1- Cement factories, high include four factories distributed from the north in Toura to the south in El-Tebeen at a distance of about 30 Km.
2- Engineering industries (Cars factory, Pipes and tubes factory).
3- Iron and steel factories.

The locations of the factories which represent the major source of air pollution at Helwan with respect to the observatory place (NRIAG), the wind direction and the percent of each direction represents the distribution of total. As it can be see, the major

source of wind direction is from the N and N-E, which represents about 50% of the total direction [9].

This means that Toura El-Cement and Helwan Portland cement factories represent 50% of the air pollution resources at Helwan. The national cement factory and iron and steel factories represent about 40% (N-W, S, W, S-W directions) of the total percent of air pollution resources at Helwan.

Fig.(1) shows the annual variation of the monthly means of intensity of global (G) and direct (I) solar radiation, spectral bands B1, B2, B3, B4. This result is not surprising and is in a good agreement with many other studies that mention a pronounced maximum in summer and minimum in winter. Fig.(2) shows meteorological parameters (relative humidity, air temperature, sunshine duration, visibility, and wind speed.

Fig.(3) shows the Linke turbidity factor in Helwan during the period 1915-1921 [10], equivalent values during 1934 [11], 1967 [12], and 1991-1995 for different month of the year, the lower curve i.e. that of 1915-1921 shows values markedly below that of 1934, 1967, and 1991-1995. This is the result of the increased air pollution in the area during recent years, as during the period (1915-1921) the area was nearly free of the industrial establishment as mentioned before. As a result of the industrialization of the area the turbidity factor was more than double (fig. 3a). For example the turbidity factor L in July 1991-1995, 1967, and 1934 was equal to 6.2, 5.4, 3.2 respectively, while during the same month in the period 1915-1921 it was 3.1. The curves in the fig.(3a) clearly indicate that the turbidity factor shows slightly monthly variation before industrialization, while marked variations are noticed in recent years i.e. after industry has spreader in the region. This is mainly due to monthly variation in pollution levels within the area in recent years.

The monthly values of β and L for Avignon, Dhahran, and Helwan plotted in Fig.(3a), indicate that the variation of the turbidity coefficients at Helwan is similar to that of Avignon and Dhahran. However, the magnitudes of the monthly values of the coefficients for Helwan are about double those of Avignon and smaller than Dhahran generally in Linke turbidity except in winter months that due to, higher values of relative humidity in winter months. With respect to Angstrom turbidity represent by a higher than Dhahran in all months except winter months because in spring, due to Khamassin dispersion with additional to air pollutants . In summer due to higher values of air temperature and wind speed which caused the diffusion in dust and aerosols from the source of air pollutants (cement factories). Winds blow from the desert area and are highly loaded with dust particles especially in spring months that increase the atmospheric turbidity throughout the year with addition to effect of air pollutants from the industrial wastes. On the other hand, Avignon is a semirural site falling in a temperate climate zone and dominated by vegetation and lack of dust storms.

Fig.(4) shows the rate of variation for Linke and Angstrom turbidity for the spectral distribution in all bands under study: high values are also observed in April, which due to the increase of dust concentration due to the occurrence of Khamssin depressions. There is a minimum for L and β in March, which characterized by clean atmosphere (especially after passage of the cold front). March can considered as a transitional month from winter regime (extratropical depressions) to spring regime (Khamssin depressions). There is also, a minimum for β in October and November. This is due to inversion of air

masses coming from Mediterranean sea, to replace the summer boundary layer loaded by dust over Helwan. In addition, This months are almost cloudless. Having the annual minimum of β, and enjoying stable weather conditions. Observation were taken in the period of June 1991 to February 1996, the number of observations totaled 475. On examining the mean values of α we found that, the value equal 1.29 closed the mean value of 1.3 suggested by Angstrom.

Fig.(1,4) shows the results which given in table (2), Angstrom turbidity shows highest degree of turbidity in B2 which demonstrate the effect of dust and aerosol. For Linke turbidity as same result that B1 and B4 has a highest degree of turbidity respectively except in January and December due to highest in relative humidity and lowest in air temperature, sunshine duration, visibility, and wind speed. The meteorological parameters effect on some of short-wave and move some to long-wave which demonstrate clear in B4 specially in January and December. Regulation result given by other bands that, B3 have lowest value and same result for B2,B3, and B4. With respect to I which denote to summation of all bands given a media level for all bands. Hence we can say that, the degree of turbidity demonstrate highest values in the band which given a high effect with dust and aerosol. Degree of Angstrom turbidity ranged from 0.1 to 0.2 in autumn and winter and from 0.15 to 0.3 in spring and summer. Relationship between Linke and Angstrom turbidity shown in fig.(5), note that B2 given highest value in Linke and Angstrom:

Table (2): Monthly mean average of global (G), direct(I), and spectral bands (B1,B2, B3), maximum(Max), minimum(Min), average($\bar{X}$), and relative of standard deviation (St. Dev.).

Parameter		Max.	Min.	$\bar{X}$	St. Dev. %
G		608	311	507.25	20
	$I_{\Delta\lambda}$	559	408	513.5	8
I	L	6.55	4.46	5.96	10
	$I_{\Delta\lambda}$	157	97	139	11
B1	L	6.9	4.71	6.21	9
	β	0.17	0.04	0.116	32
	$I_{\Delta\lambda}$	68	47	62.7	8
B2	L	7.57	4.5	6.49	13
	β	0.282	0.14	0.21	19
	$I_{\Delta\lambda}$	47	33	41.12	7.3
B3	L	6.11	3.98	5.4	10
	β	0.24	0.11	0.191	21
	$I_{\Delta\lambda}$	287	231	269.83	5
B4	L	7.19	3.39	6.16	16

$I_{\Delta\lambda}$ = denotes the spectral irradiance observed at the instrument in the same spectral interval

Fig.(5) shows the relationship between Linke and Angstrom factors at Helwan represented by:

Band	Equation	CC%	RMS.	
B1	$\beta = -0.186 + 0.048\ L$	66	0.19	(11)
B2	$\beta = -0.270 + 0.073\ L$	81	0.24	(12)
B3	$\beta = -0.076 + 0.049\ L$	67	0.19	(13)

The relationship of equ.(9) is similar to the model reported for Avignon (France)[13];

$$\beta = -0.103 + 0.052\ L \qquad (14)$$

and to the relationship of Potsdam (Germany)[14];

$$\beta = -0.100 + 0.05\ L \qquad (15)$$

It is observed from Fig.(6) which given monthly mean variation of Angstrom and Linke turbidity at different spectral bands, that medium size particles of the B2 band contribute more to the extinction effect, followed by the large particles of the B4 band, and then by other small and medium particles of the bands B2 and B3.

Based on the definitions of G and β & L, a typical was made to correlate them by a Linear regression relation. It was demonstrate from Fig.(6), found that:

		CC%	RMS.	
I	$L = 3.454 + 0.00483\ G$	89	0.2010	(16)
B2	$L = 2.300 + 0.00826\ G$	90	0.0640	(17)
B2	$\beta = 0.015 + 0.00038\ G$	89	0.0005	(18)

The values of Angstrom and Linke turbidity are high in afternoon than beforenoon, because the source of pollutants almost in North-east and North in wind direction.

6- CONCLUSION

The Linke turbidity factor L, and Angstrom turbidity coefficient β, were obtained from the spectral measurements of radiation. The summer varies of these coefficients were found to be larger than their winter values. The urban climate represented by Helwan showed to have higher L and β values compared with the semirural climate represented by Avignon (France) and Lower values of L but the higher order of β compared with the desert climate represented by Dhahran (Saudi Arabia).

The results reported here suggest that there is a significant decrease in attenuation by aerosols and particles with wavelength. The Angstrom turbidity coefficient can be taken equal to the attenuation at the wavelength B2 which ranged from 530 to 630nm. The Linke factor L, and Angstrom coefficient β, were obtained from the radiation measurements. The summer values of these coefficients were found to be larger than their winter values. The desert climate represented by Helwan showed to have higher L value compared with the observations which taken at the same site. Spectral distribution of

different bands from I to B4 showed a variation within the regression coefficients between β and L.

The atmospheric turbidity for a Helwan region is highly dependent on wastes of industrialization and the weather activities in that region (i.e., wind speed, wind direction, air temperature, and humidity); three factors can be advanced to explain this behavior: Winds origin; north, north-west winds, which are the more turbid are more frequently observed in summer than in winter. The air temperature: higher temperature in summer, enhancing vertical convection and particle, can induce more turbid atmosphere. The water vapor content: high humidity can induce growth and development of water droplets. In our case: air mass origin plays the most important contribution in the atmosphere turbidity and humidity are secondary factors, with only limited effects

It is established that, there are a good relationship between global solar radiation with Angstrom and Linke turbidity factors at Helwan.

REFERENCES

[1] J.M.Pinazo,J.Canada, and J.V.Bosca, "A new method to determine Angstrom's turbidity coefficient: its application for Valencia", Solar Energy, Vol. 54, No. 4, pp.219-226, (1995).

[2] W.D.Sellers, "Physical climatology University of Chicago Press, Chicago" (1965).

[3] H.S.Sahsamanoglou and A.A.Bloutsos, "Cleansing of the atmosphere in the Athens area by means of rainfall and wind: The impact of climate planning and building", Elsevier Sequoia, 125-128 (1982).

[4] M.A.Abdelrahman, S.A.M.Said, and A.N.Shuaib,"Comparasion between atmospheric turbidity coefficients of desert and temprate climates", Solae Energy, Vol. 40, No.3, pp. 219-225(1988).

[5] WMO- "International operations Handbook for measurement of back ground atmospheric pollution", No.491(1978)

[6] WMO "Operations manual for sampling and analysis techniques for chemical constituents in air and precipitation", No. 299, Geneva- Switzerland (1974).

[7] K.L.Coulson, "Solar and terrestrial radiation", Academic Press, New York (1975).

[8] Moslam Shaltout,"Solar radiation and air pollution in Cairo", Proceedings of the third Arab International Solar Energy Conference, Baghdad-Iraq, Edited by N.I.Al-Hamadani and et.al., pp.53-58, 21-24, Feb., (1988).

[9] A.H.Hassan, "Environments and their effects on the photovoltaic performances in the desert climate of Egypt", Ph.D. Thesis, Faculty of Science, Menofia University (1995).

[10] H.Knox-Shaw, "Observations of solar radiation 1915-1921", Helwan Observatory, Physical Department, Fouad University, Egypt Bulletin No.23(1951).

[11] A.Jaenicke, and F. Kasten, "Estimation of atmospheric turbidity from the burned traces of the Campell-Stotokes sunshine recorder", Applied Optics, Vol. 17, No.16, pp.2617-2621(1978).

[12] N.A.Higazy, "Effect of air pollution visibility and penetration of solar ultraviolet radiation", Ph.D. Thesis, Faculty of Science, Cairo University (1973).

[13] M.Katz,A.Baille, and M.Mermier,"Atmospheric turbidity in semi-rural site-1, evaluation and comparison of different of different atmospheric turbidity coefficients", Solar Energy, Vol. 28, No. 4, pp.323-327 (1982).
[14] H.Hinzpeter, Ueber Trubungsbestimnungen in Postdam in den Jahren 1946 und 1947. Zeit. Fur Meteor. 4, 1(1950).

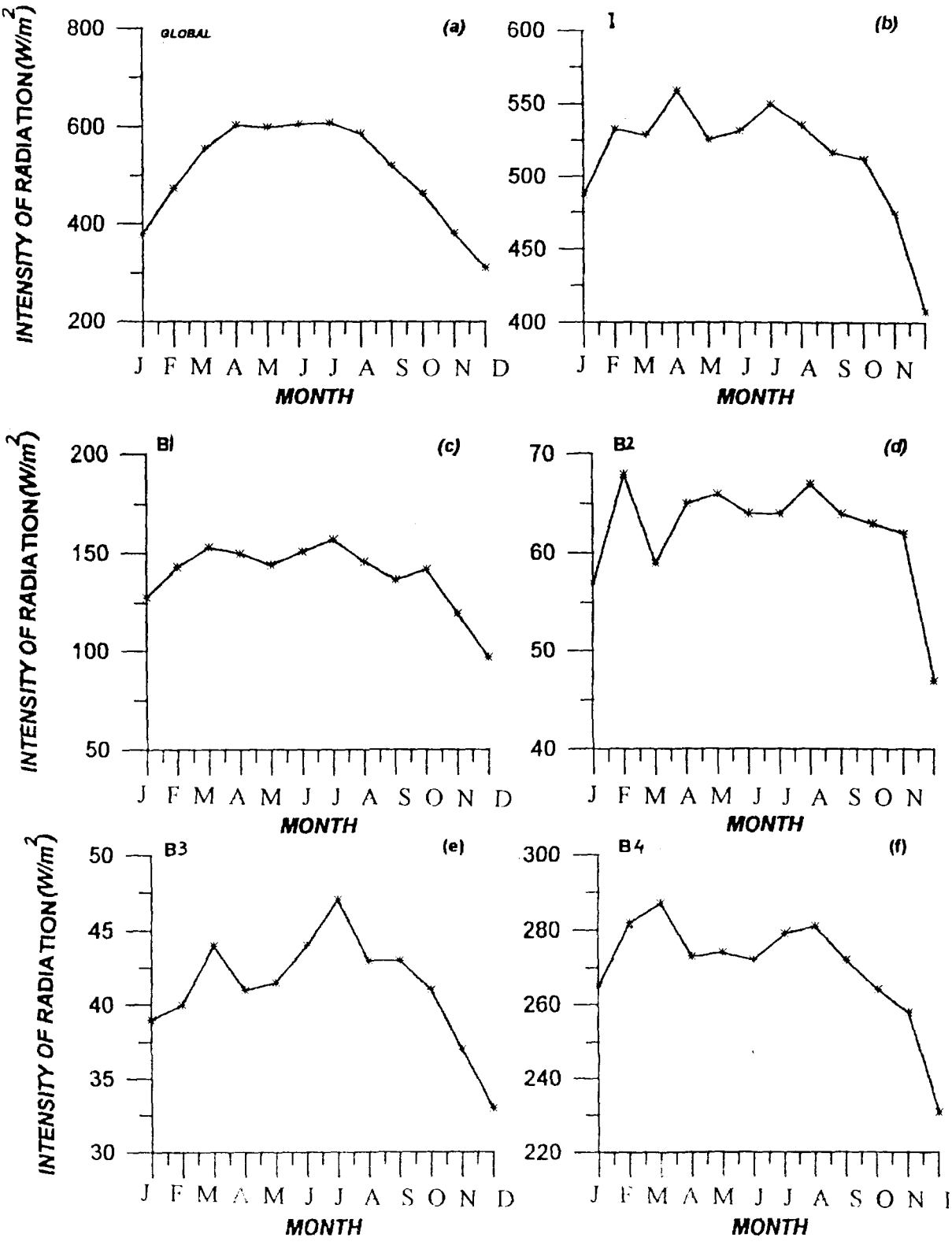

Fig.(1) : Monthly mean of global (a), I(b), spectral bands B1 [350-530 nm], B2 [530-630 nm], B3 [630-695 nm], and B4 [695- 2 800 nm]at Helwan from June 1991 to February 1995.

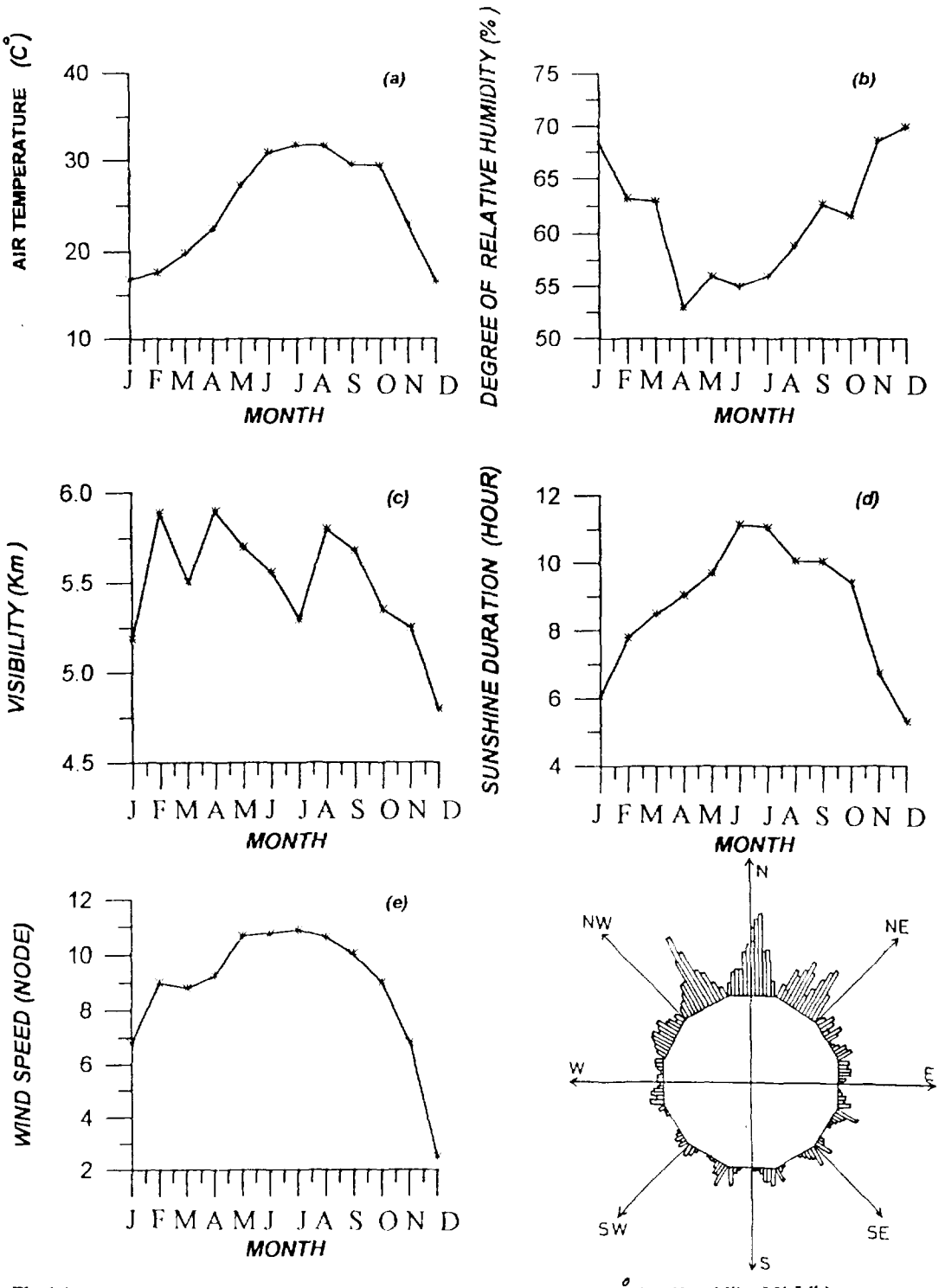

Fig.(2) : Monthly mean of meteorological parameter Temperature [C°] (a), Humidity [%] (b) ,Visibility [Km] (c), Sunshine duration [hour] (d), wind speed (node) (e) and wind direction (f) at Helwan from June 1991 to February 1996

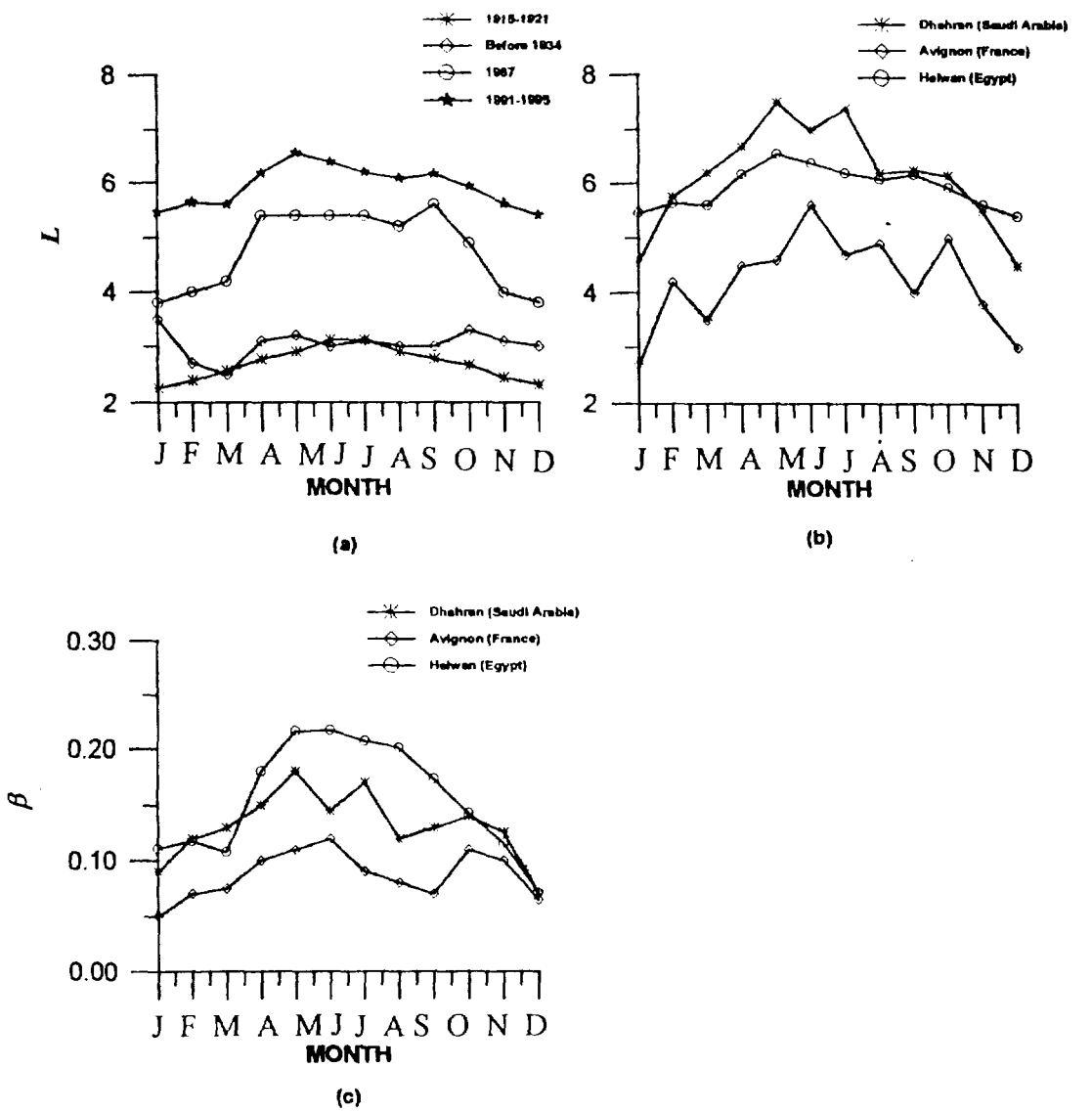

Fig.(3): Comparison between Linke turbidity [L] at different years at Helwan (a), between Linke turbidity at different regions(b), and between Angstrom turbidity [β] at different regions(c).

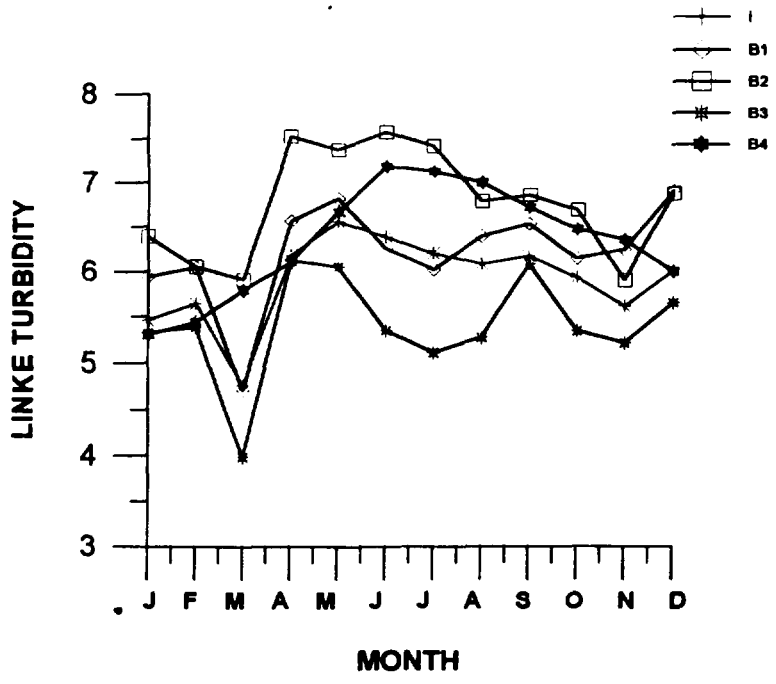

(a)

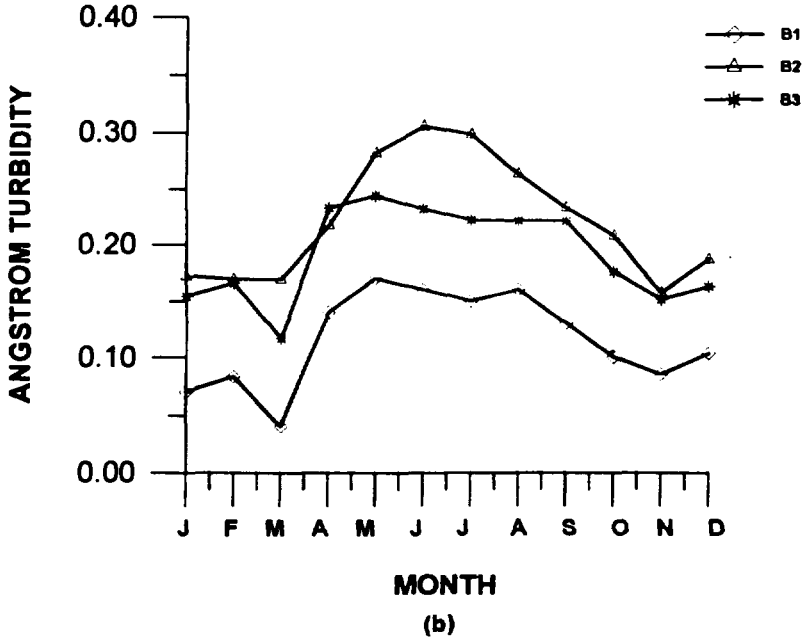

(b)

Fig.(4): Monthly mean variation of Linke (a) and Angstrom (b) turbidity at different spectral bands at Helwan From June 1991 to February 1996.

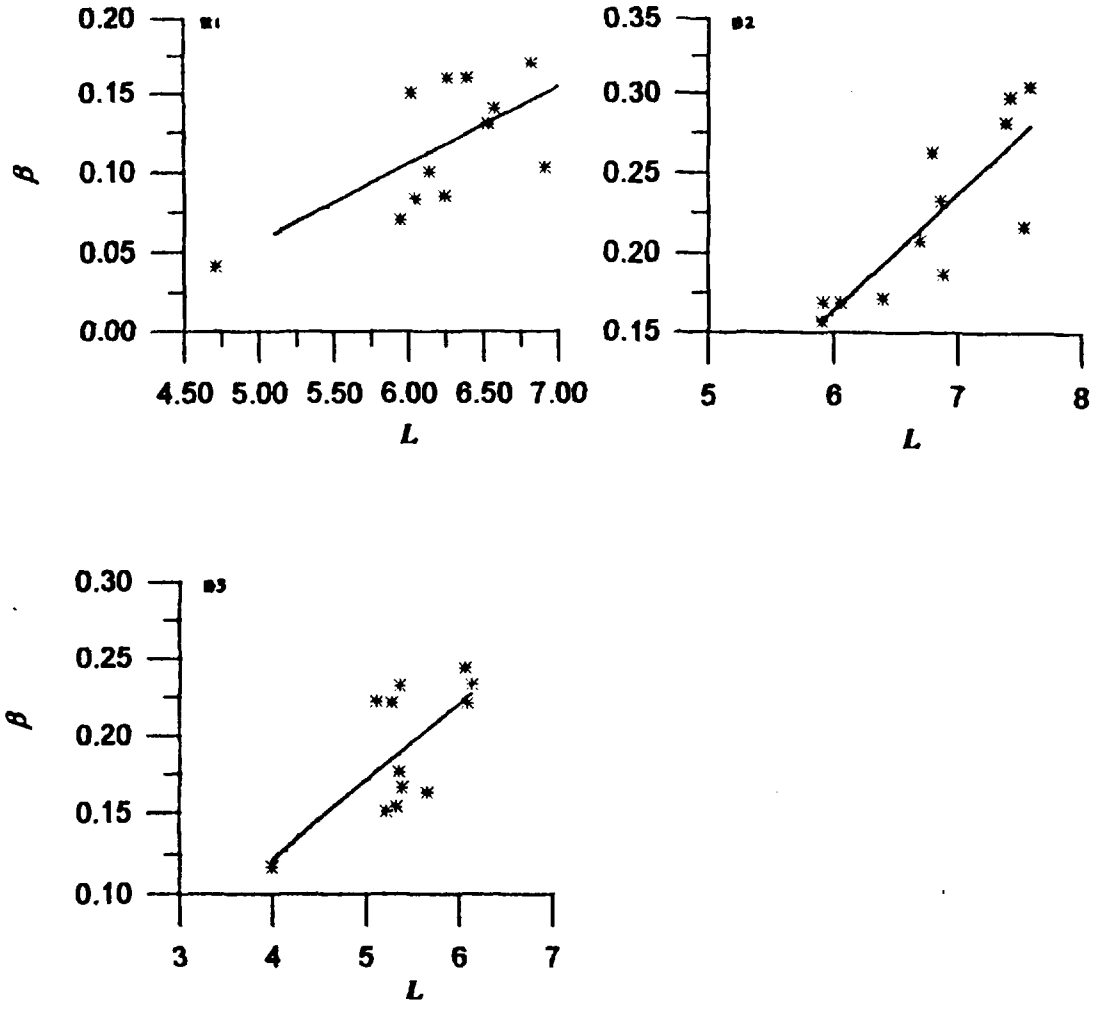

Fig.(5): Relationship between Angstrom turbidity[β] and Linke [L] turbidity in different spectral bands at Helwan

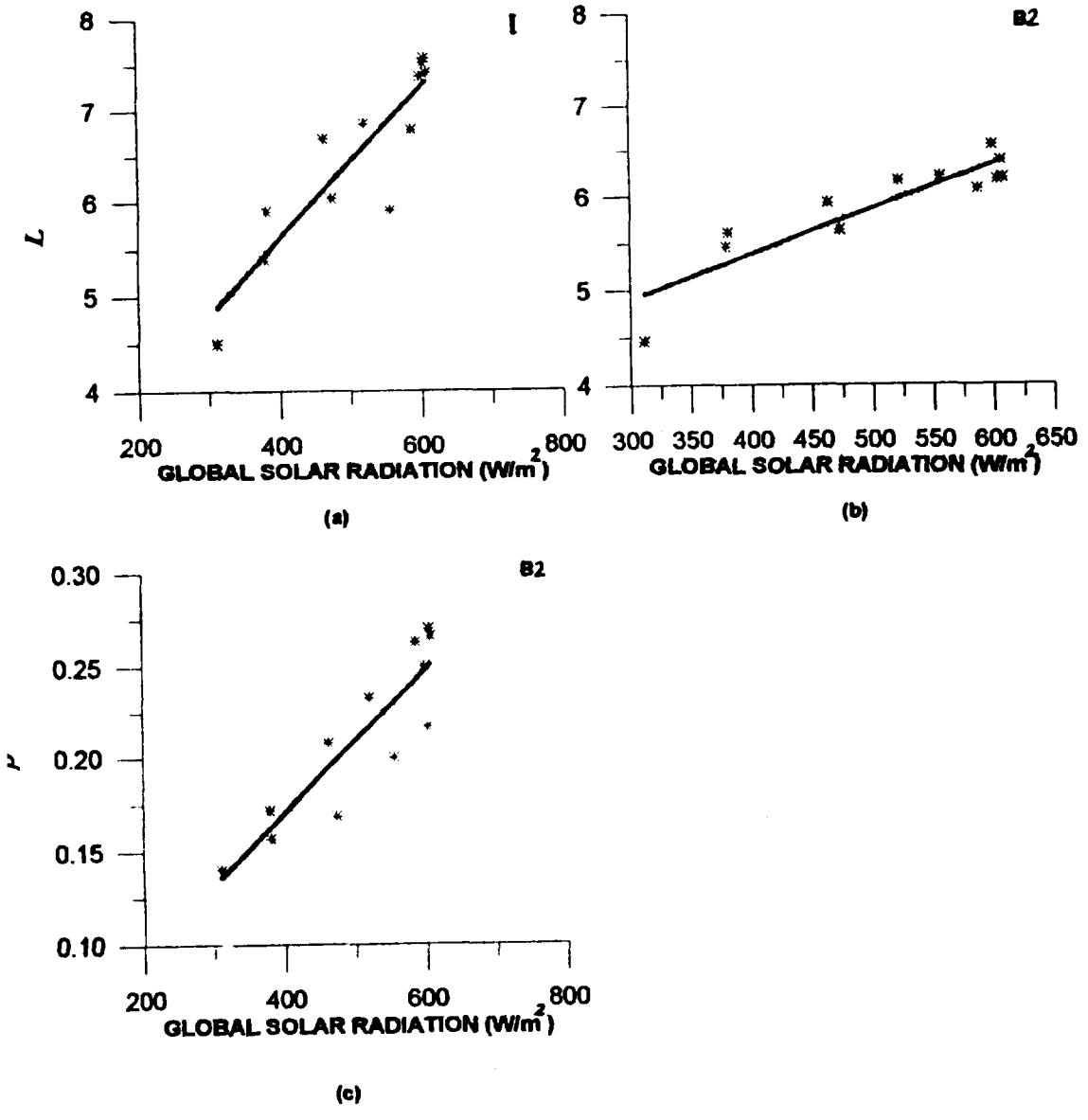

Fig.(6): Relatioship between Linke turbidity [L] at I(a) & B2 (b), and Angstrom turbidity [β]at B5 (c) with global solar radiation (W/m^2) at Helwan from June 1991 to February 1995.